Evolution of 4π observables in the Vlasov-Uehling-Uhlenbeck theory and the transverse momentum transfer as a barometer for hadronic matter

Joseph J. Molitoris* and Horst Stöcker
Institut für Theoretische Physik, J.W. Goethe Universität, D-6000 Frankfurt am Main, Federal Republic of Germany

Brian L. Winer
Physics Department, University of California, Berkeley, California 94720
(Received 22 December 1986)

We study the dynamics of high energy heavy ion collisions through the Vlasov-Uehling-Uhlenbeck approach. Equilibration is observed, for central collisions. It is shown that the produced entropy, the pion multiplicity, flow angle, and transverse momentum distributions saturate at the moment of maximum compression and temperature. The effects of the nuclear equation of state and the Pauli principle are investigated. For the flow angle distribution there is a 20 deg reduction of the peak flow angle due to the Pauli principle. A stiff equation of state results in a 10—20 deg increase over the soft equation of state at all energies. The transverse momentum at projectile rapidity exhibits a peak structure as a function of impact parameter b. A 40% difference between soft and hard equation of state is observed for the peak impact parameter, i.e., for intermediate multiplicities.

One of the most important problems of high energy heavy ion physics is to find observables which can be linked unambiguously to the properties of the hadronic matter at its densest and most excited (and exciting) state. Unfortunately, this state prevails only for a very short time $t \approx 10^{-23}$ s.

It has been argued that the collective flow, p_x, probes the pressure $P(\rho,T)$ built up in the collision, which is largest at the highest density and temperature; hence $p_x \approx P(\rho,T)^{\max}$. It was therefore proposed to use the collective flow effects as a "barometer" to extract information on the nuclear equation of state.[1]

The total pion multiplicity, on the other hand, is (in a simple thermal model) related to the thermal energy per nucleon E_t. It could be used as a "calorimeter," and once the collective flow energy in the moment of pion freeze-out is known, we would have a direct measurement of the compression energy.[2] Neither the flow nor the pion data yield *direct* information on the achieved maximum density.

However, fragment yield ratios (e.g., d/p) depend on the entropy created in the collision.[3] Note that once the thermal energy is known, the entropy S/A can be used to obtain the density: the entropy is related to the density in phase space, and once the temperature is known, integration over momentum space can be used to find ρ. Unfortunately, S depends only logarithmically on the density. Therefore, small differences in ρ can be very difficult to get at. By measuring complex particles, the sensitivity to ρ could probably be enhanced.

In addition, the fragment spectra need to be known to determine the degree of thermal equilibration. Thus only the simultaneous measurement of flow, pion yield, and fragment yields can give detailed information of the state of the system. This is why exclusive experiments with a wide dynamic range are necessary for probing dense nuclear matter.

In the present paper we want to demonstrate that the operational procedure described above (which was developed on the grounds of macroscopic, thermal equilibrium theories like nuclear fluid dynamics) is in accord with the microscopic Vlasov-Uehling-Uhlenbeck (VUU) theory,[4] which explicitly treats nonequilibrium and quantal effects, as well as the nuclear equation of state. This theory has been successful in predicting the flow effects and pion yields observed in the first round of 4π experiments.[2,5] Evidence for a surprisingly stiff (i.e., repulsive) nuclear equation of state has been reported.[1,2,4,6]

First let us remind ourselves of the VUU equation:

$$\frac{\partial f}{\partial t}+\mathbf{v}\cdot\frac{\partial f}{\partial r}-\nabla U\cdot\frac{\partial f}{\partial p}=-4\int\frac{d^3p_2d^3p_1'd\Omega}{(2\pi)^3}\sigma(\Omega)v_{12}[ff_2(1-f_1')(1-f_2')-f_1'f_2'(1-f)(1-f_2)]\delta^3(p+p_2-p_1'-p_2')\ .$$

The two most important terms in this equation are the potential $U(\rho)$ and the Pauli corrected scattering integral. Let us discuss the relevance of these terms separately. From now on we will loosely refer to the soft, S, and hard, H, equation of state (EOS), respectively, when we mean the two Skyrme forms of the local potential[4]

$$U(\rho)=-a\rho+b\rho^{\gamma}\ ,$$

with $\gamma=\frac{7}{6}(S)$ and $\gamma=2(H)$, respectively.

Momentum dependent interactions have not been included into the present calculations; it has recently been shown[6] that they are quite important for the quantitative analysis of flow and particle (π,K) production.

The total energy of cold nuclear matter, i.e., the potential energy plus kinetic energy per nucleon, which correspond to these two local potentials are depicted in Fig. 1. The soft EOS coincides with results of nuclear matter calculations.[7] Also shown is a supersoft EOS, which seems to be required to achieve successfully supernova explosions.[8] Observe that the hard EOS yields a 15 and 60 MeV/nucleon higher compressional energy at $\rho/\rho_0=2$ and 3, respectively, than the soft EOS. In the following we will examine the influence of the EOS on the collision dynamics.

The most obvious effect of the EOS is the binding, given to the nuclei: Figures 2 and 3 show the time evolution for the ground state of Ca and Nb nuclei at rest. Observe that both the configuration space and momentum space distributions are preserved reasonably well over time scales compatible to typical collision times at high energies, $t\simeq 40$ fm/c. [There is a small (less than 10%) evaporation of particles unbound in the present scheme.] The treatment of binding is important for collective flow effects; the intranuclear cascade model,[9] which lacks dynamic flow effects, can produce spurious flow angles as large as 20° if the binding is neglected.[10]

Snapshots of VUU calculations are shown in Fig. 4 for the system Nb (400 MeV/nucleon) + Nb at three different impact parameters, $b=1$, 3, and 5 fm. Observe that the system is in a highly compressed state at $t\simeq 10$ fm/c. This dense compound decays rapidly, with a preferential sideward flow away from the beam axis; the sideward flow effect is clearly the largest at the smallest impact parameter, since there, also, the total amount of

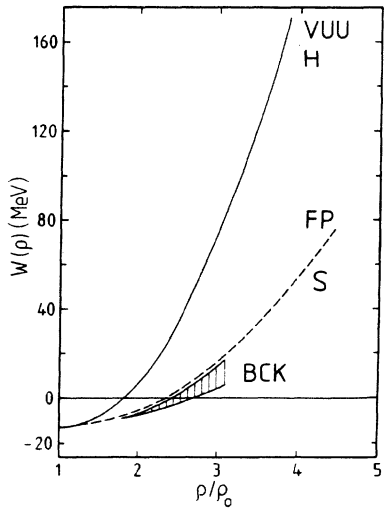

FIG. 1. The hard and soft EOS's used in the VUU calculations, denoted VUU and FP, respectively, as compared to the BCK-EOS (Ref. 8).

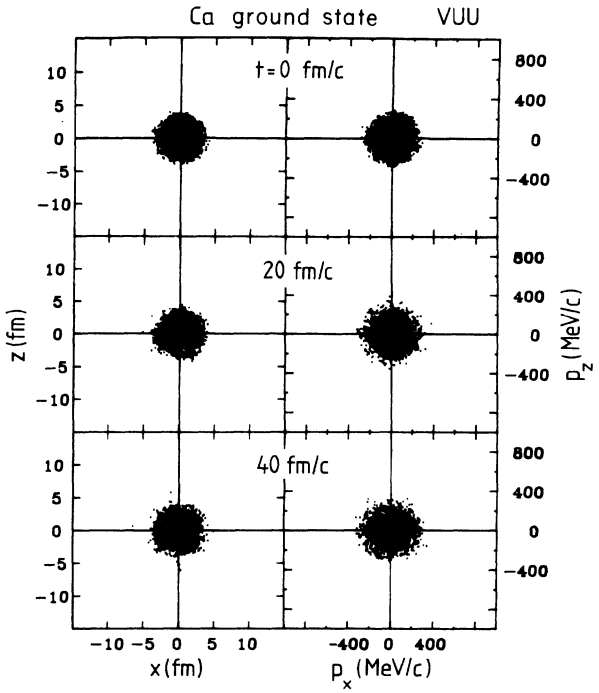

FIG. 2. Time evolution of Ca nuclei at rest in configuration (left) and momentum space (right). This figure demonstrates the stability of the nuclei in the VUU approach.

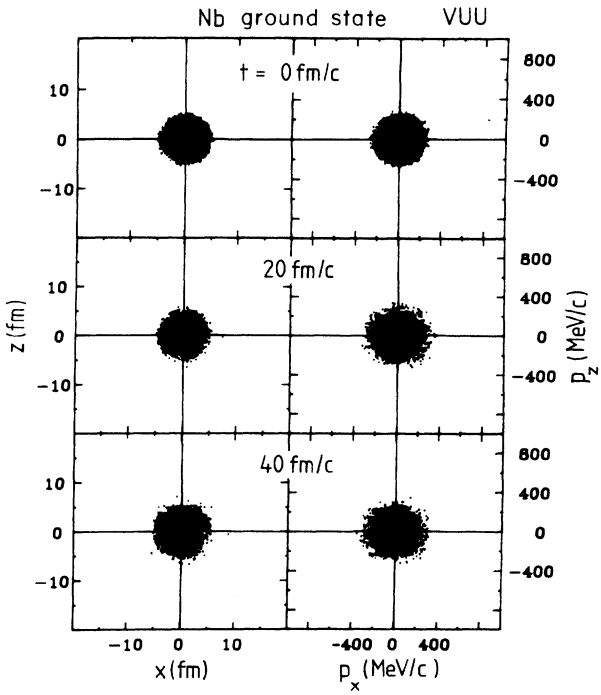

FIG. 3. Same as Fig. 2, but the stability of Nb nuclei is shown.

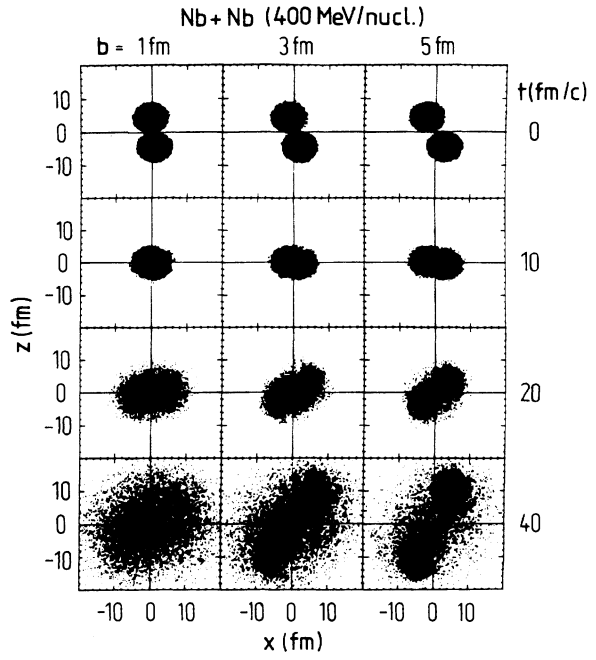

FIG. 4. Time evolution of the single particle distribution function in configuration space for the system Nb (400 MeV/N) + Nb at three impact parameters.

compressed matter is the highest. We will come back to the flow effects in a moment.

Figure 5 shows the time dependence of the density in a test sphere of radius $r=3$ fm around the origin of the c.m. system for the $b=3$ fm case. Observe the rather short ($\simeq 10$ fm/c) duration of the high density stage and the rapid subsequent expansion. This shows that high energy heavy ion collision can indeed be useful for producing high density nuclear matter. But can we also study the nuclear equation of state in these reactions? For this to be possible we must prove that the longitudinal momentum is equilibrated and that for the participants, local thermal equilibrium is approached. This is the central prerequisite for the validity of fluid dynamics.

Figure 6 shows momentum space snapshots for the same system as in Fig. 4. We would like to emphasize that a nearly isotropic distribution of all nucleons is observable at $t=20$ fm/c for $b=1$ fm, with a small remaining longitudinal momentum excess reflecting the spectator remnants. For the larger impact parameters, i.e., at smaller geometrical overlap, there are fewer participants. They can still come close to thermal equilibrium while the *spectators* do *not* equilibrate. How does this behavior change when going to high energies? Figures 7 and 8 show the configuration— and momentum space snapshots for the system Nb (1050 MeV/nucleon) + Nb at the same impact parameters as in Fig. 4. Note that the higher incident longitudinal momenta are as effectively equilibrated as at the lower energy. However, the spectator fragments are now much more separated in momentum space, and therefore there is a clear forward-backward stretched momentum distribution, which, in fact, results in reduced flow angles at high energy. This will be discussed extensively below (this reduction occurs in spite of the observed increase on the transverse momentum transfer).

Figures 9 and 10 show the time evolution of the most characteristic observables for the system Nb (1050 MeV/nucleon) + Nb in a typical "central" collision ($b=3$ fm). The density and temperature represent ensemble averages over 75 events and have been obtained in a test sphere of radius 2 fm around the origin in the c.m. system.

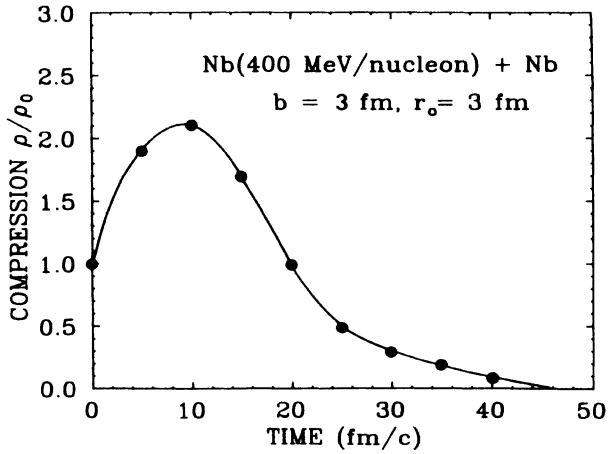

FIG. 5. Time evolution of the central density in the same reaction as in Fig. 4, in a test sphere of radius 3 fm.

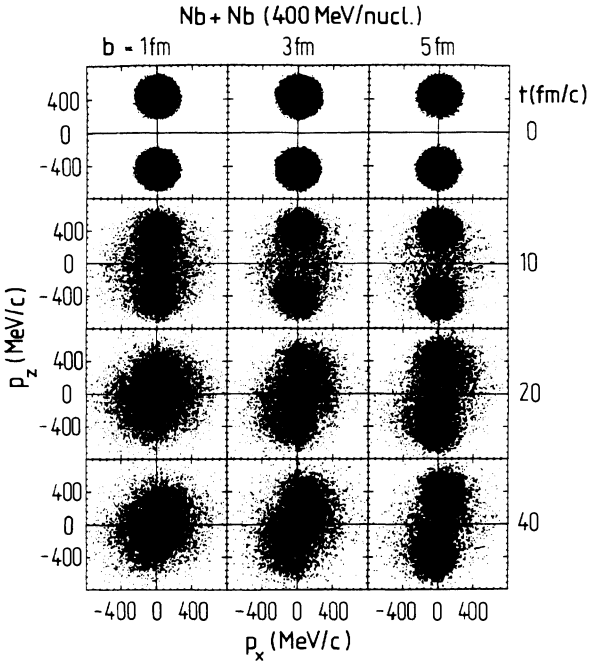

FIG. 6. Same as Fig. 4, but in momentum space.

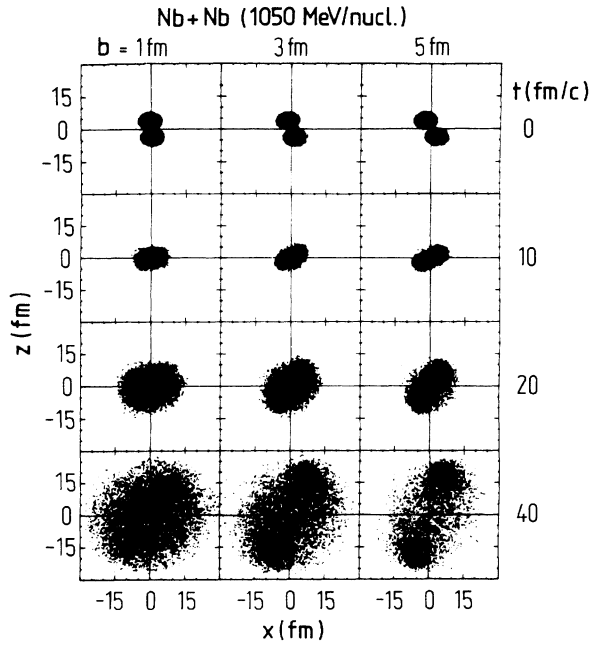

FIG. 7. Same as Fig. 4, but at 1050 MeV/nucleon.

The central density rises quickly (in 5 fm/c) to its maximum value, $\rho/\rho_0=2.7$, then drops exponentially, falling below ρ_0 at 15 fm/c and below $0.5\rho_0$ by $t=17$ fm/c. The simple one dimensional fluid dynamic shock model[1] with the same stiff EOS predicts a density of $2.9\rho_0$, very similar to that achieved in the present microscopic VUU approach.[4] The density reached in Ar + KCl, Nb + Nb, and Au + Au collisions is nearly identical. It is shown as a function of energy for the H and S EOS in Fig. 11. It is

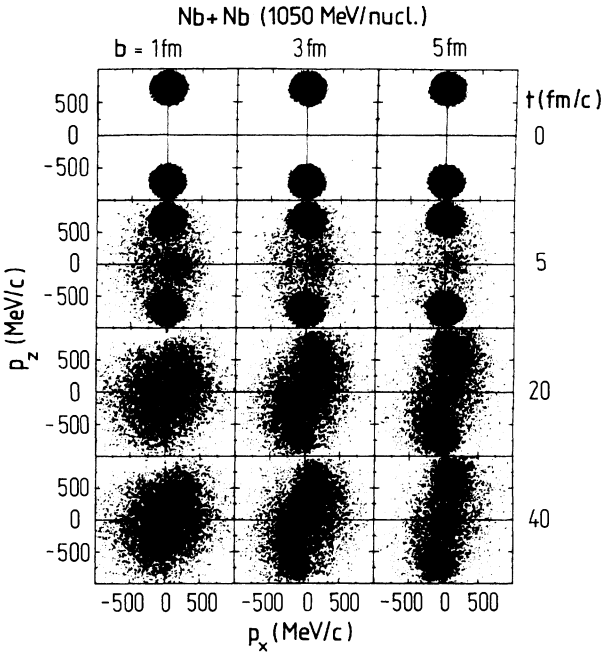

FIG. 8. Same as Fig. 7, but in momentum space.

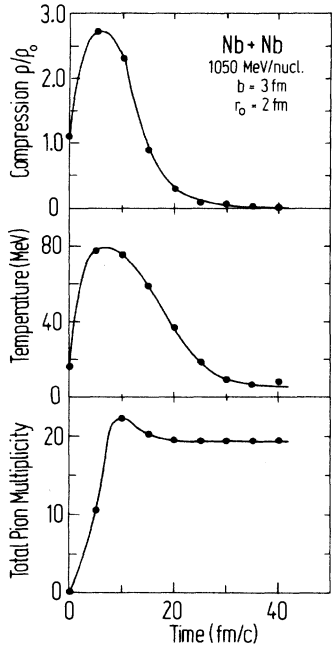

FIG. 9. Time evolution of the density, temperature and total pion yield for the reaction shown in Figs. 7 and 8. Note that the pion yield reaches its asymptotic value at the moment of highest density and temperature.

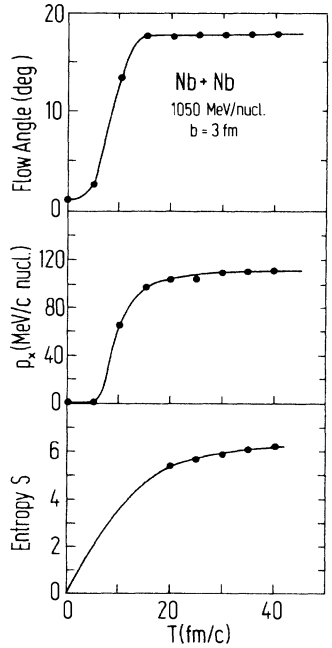

FIG. 10. Time evolution of the flow angle, transverse momentum, and entropy for the same reaction as shown in Fig. 9. Note again that the asymptotic values are reached when the point of highest density and temperature is observed (Fig. 9).

interesting that the maximum density does not depend much on the atomic number, but it does depend strongly on the EOS. About a half a unit higher densities are achieved with the soft equation of state at energies between 0.4 and 2 GeV/nucleon (see Fig. 11). The densities achievable are much lower in the VUU model than those reached with the intranuclear cascade model: the compression energy there is neglected entirely and the cascade predicts $(\rho/\rho_0)_{\max}=4.0$ at 1050 MeV/nucleon.[9]

We calculate the "temperature" in the present theory via the transverse momentum average from the thermodynamic relation[11] $\langle p_\perp^2 \rangle = 2mT$ in a central sphere of radius 2 fm. The temperature also rises rapidly, approaching $T=80$ MeV by $t=9$ fm/c (see Fig. 9). This temperature also compares quite well with the value of 78 MeV extracted from the simple shock model.[4] Since the "hot," i.e., highly energetic, particles are quickly transported out of this central zone, the temperature drops rapidly.

It reaches values $T\approx 35$ and 15 MeV at $t=20$ and 25 fm/c and drops to very low values $T\langle 10$ MeV for $t\rangle 30$ fm/c, in spite of the high incident energy of 1 GeV/nucleon studied here. The temperature of the system drops everywhere to these low values; we witness the rapid expansion of the system, which leads to strong correlations between momentum space and configuration space: at each point in space the *co-moving* momentum distribution becomes narrower, i.e., the temperature is lowered. This is a result of Liouville's theorem, which holds in the VUU theory once the N-N collisions cease, i.e., when the free streaming case is reached. Simultaneously, the system picks up collective flow energy to which we will return in a moment. Note that the low temperatures predicted in the present theory for the late stage of the reaction are in accord with the results of fluid dynamical calculations;[1] they also result from a quantum statistical analysis of the fragment yields, which gives $T\leq 20$ MeV at 1 GeV/nucleon.[3,12]

At these temperatures, the densities are of the order of $\rho/\rho_0\simeq\frac{1}{4}-\frac{1}{10}$. It is only at these late times that the nucleon-nucleon collisions cease, i.e., the formation of fragments is established and the so called fragment freeze-out point is reached.

Figures 4 and 6–8 show one other important aspect which we would like to turn to now: the single particle distribution function is initially tightly confined to the projectile and target. However, due to the large number of elementary scattering processes in the reactions, there occurs a rapid spreading of the single particle distribution function over phase space during the stopping and equilibration stage. Hence, the total volume in phase space occupied by the same number of particles is not conserved—as it would be in classical dynamics in accord with Liouville's theorem. The increase of the volume in phase space expresses the creation of entropy.

The entropy is expected to saturate in the adiabatic expansion. For the simple case of noninteracting fermions, one has

$$S=-\int d\Gamma[f\ln f+(1-f)\ln(1-f)]\ ,$$

where $d\Gamma=[4/(2\pi)^3]d^3r\,d^3p$ is the phase space element and f is the average occupation number. To evaluate the entropy of the nucleons, one must thus calculate a six dimensional integral. We use r, p, and Θ_{pr} as the appropriate variables.[13]

It has been demonstrated in Ref. 14 that this method[13] overestimates the entropy by about one unit. The time development of the uncorrected entropy is shown in Fig. 10. Figure 12 shows the bombarding energy dependence of the uncorrected entropy for the system Au + Au at $b=3$ fm. If corrected by the method of Ref. 14, the entropy values calculated agree well with the entropy extracted from the data[12] via quantum statistical calculations.[3]

In contrast to the fragment freeze-out, which occurs at temperatures $T<30$ MeV, we find that the pions freeze out during the highest temperature stage of the collision, $T=80$ MeV, as can be seen in the lowest part of Fig. 9.

Pions of different isospin are created in the VUU approach through the elementary NN↔NNπ channel and through the Δ resonance. Both production and absorption

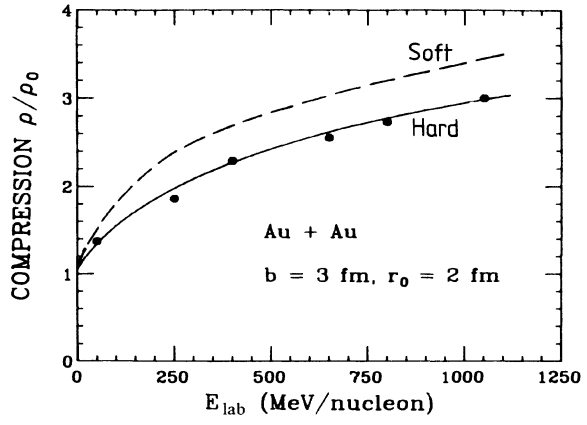

FIG. 11. The maximum density versus bombarding energy for the hard and soft EOS's for the system Au + Au.

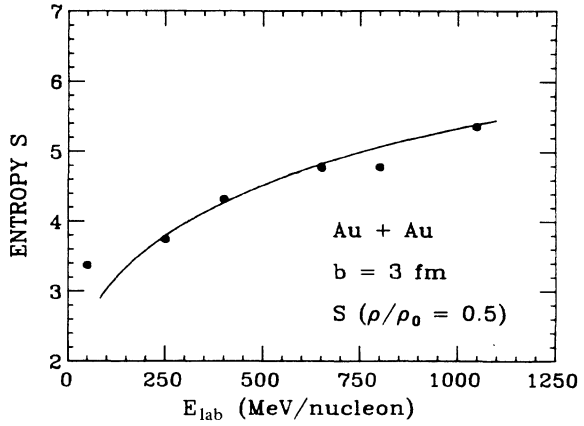

FIG. 12. The uncorrected entropy is shown for the Au + Au system as a function of bombarding energy.

mechanisms are treated microscopically. The pion number rises to a maximum value at $t=10$ fm/c, which is only about 10% above its asymptotic final value.

The fact that the pion yield approaches its asymptotic value at a somewhat earlier time than the moment of highest compression demonstrates that information on the high density stage can be gained from the pion multiplicity. It has been shown that the pion yield can give the thermal energy, the compression energy, and the temperature in the moment of the pion freeze-out,[2] if the thermal energy of the hadrons is treated as a free gas.

However, it has recently been shown[6] that momentum dependent interactions in the VUU and quantum molecular dynamic approach can drastically alter the pion yields as well as the kaon yields, which show qualitatively the same time dependence as the pions; the extraction of the EOS from pion yields is rendered difficult.

Furthermore, the coupling constants of the delta to the meson fields and, therefore, the effective mass of the delta in the medium are not known well enough to calibrate this "thermometer" with sufficient precision to infer the nuclear equation of state from the pion and kaon yields. The pion yield is shown for the systems Nb + Nb in Fig. 13. There is a strong dependence of the ratio of the π^+ and π^- yields on the Z/A ratio of the system considered. The excitation function of the π/A ratio is shown for central collisions of La + La in Fig. 14. The calculations have employed the hard local potential without momentum dependent interactions and are compared to cascade model predictions and to the recent streamer chamber data of Harris *et al.*[15]

The agreement of the present VUU results with the streamer chamber data is quite satisfactory. A similar agreement was found before for the system Ar + KCl.[2,4] It is important that the π/A ratio observed is the same for $A_1=A_2=40$ (Ar) and 140 (La), which is also obtained in the present VUU calculations. However, we know from Ref. 6 that momentum dependent interactions can yield an even stronger reduction of the pion yield than a hard local potential.

Therefore, we must study the collective flow effects in

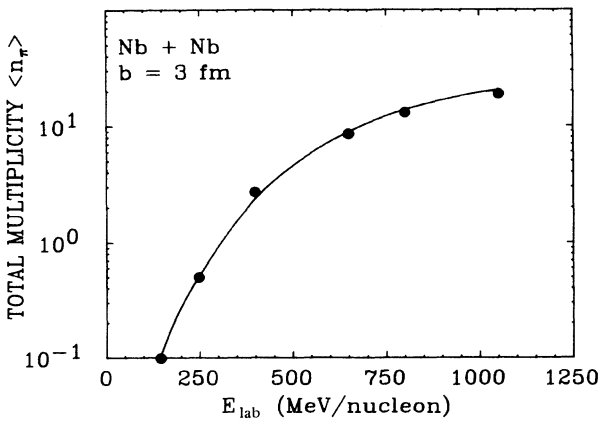

FIG. 13. The total pion multiplicity is shown for the system Nb + Nb at $b=3$ fm as a function of $E_{\rm lab}$. The H EOS has been used.

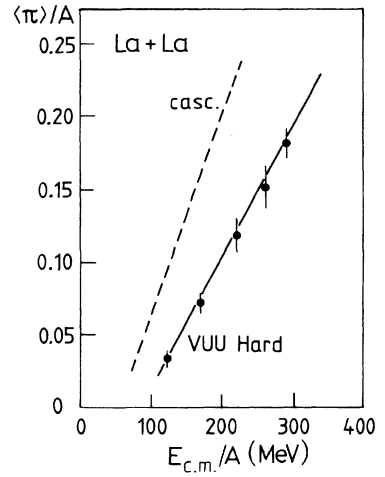

FIG. 14. The same as Fig. 13, but for the system La + La at $b=0$. The data are also shown (Ref. 15).

detail if we want to proceed towards the nuclear matter properties at the high density stage. In the course of the reaction the various momentum components develop quite differently: the longitudinal momentum starts at its maximum value and then decreases, whereas $\langle p_y \rangle$ and $\langle p_x \rangle$ start at zero and gradually build up. On first glance it seems that experimentally one can only distinguish between $p_\perp$ and p_z. However, a distinction between p_x, the transverse momentum in the scattering plane, and p_y, the out of plane momentum, can be obtained in an event-by-event analysis: both the kinetic energy flow method[16] and the directed transverse momentum analysis[17] yield the reaction plane (say, the $x-z$ plane) with good precision from a simultaneous measurement of the momenta of all the fragments in a single collision.

The kinetic energy flow tensor[16] is given by

$$F_{ij}=\sum_\nu p_i(\nu)p_j(\nu)/2m(\nu)\ ,$$

where the sum is over all charged particles in a given event and the (i,j) represent the Cartesian components (x,y,z). By diagonalizing this tensor the three principal axis can be found which define the scattering plane, the shape of the ellipsoid in momentum space, and the flow angle Θ_F for each event separately.

The time dependence of this peak flow angle is shown for the Nb(1050 MeV/nucleon) + Nb system in Fig. 10. We want to point out that the peak flow angle saturates at its asymptotic value $\Theta_F=18°$ by $t=15$ fm/c. The compression of the hot central region reaches its maximum value earlier: at that time the collective energy is largely stored in compressional and thermal energy. The compressional and thermal energy are then converted into collective flow energy, much in analogy to a compressed spring which expands and thus transfers momentum. Therefore, it takes some time for the final momentum distribution to be established. This effect is responsible for the nice one-to-one relation observed between the flow angle and the equation of state discussed below.

The second variable in use to analyze the collective flow

in nuclear collisions is the directed transverse momentum method:[17] here the reaction plane in each event is determined by finding the plane at which the out of plane momenta cancel both in the forward and backward rapidity region of the center of mass system separately. It turns out that the plane defined by the forward emitted particles agrees nicely with the backward plane, i.e., the scattering plane is well defined. Once the scattering plane is known, the average of the in-plane transverse momentum per nucleon p_x can be plotted as a function of the rapidity y. $p_x(y)$ exhibits two extrema, one at the projectile rapidity y_p and one at about the target rapidity y_T. $p_x(y_{\text{c.m.}})$ is always equal to zero because of symmetry. For very central collisions, this analysis loses its usefulness, since $p_x(y) \equiv 0$ everywhere because of axial symmetry.

Both F_{ij} and $p_x(y)$ represent a reduction of the information contained in an event-by-event analysis—the full information is contained in the triple differential cross section $d^3\sigma/dp_x dp_y dp_z$.[1,18] The triple differential cross section can be plotted for each fragment species as a function of impact parameter once the reaction plane is known, e.g., from the $p_x(y)$ analysis. The time evolution of the projection of the triple differential cross section into the reaction plane is directly observed in Figs. 6 and 8. Observe the rapid depopulation of the projectile and target momentum region for near central collisions. Projectile and target are nearly completely consumed in the intermediate rapidity participant region by $t \approx 10$ fm/c.

At large impact parameters, the increase in the number of spectators goes hand in hand with the rapid stopping and thermalization of the nucleons in the participant region. Observe that the momentum distribution is substantially tilted towards a flow angle of $\Theta_F \approx 20°$. We would like to point out again that the flow effects look even more dramatic at lower energies—this is due to the smaller initial separation of the projectile and target in momentum space. However, the flow effects for the participant particles increase at *higher* energies as a result of the higher compression achievable.

Let us now turn to the dependence of the flow angle and the transverse momentum on the EOS and on the Pauli principle. Figure 15 shows for Nb + Nb the fraction of Pauli blocked collisions (PBF) over all attempted collisions versus the bombarding energy.

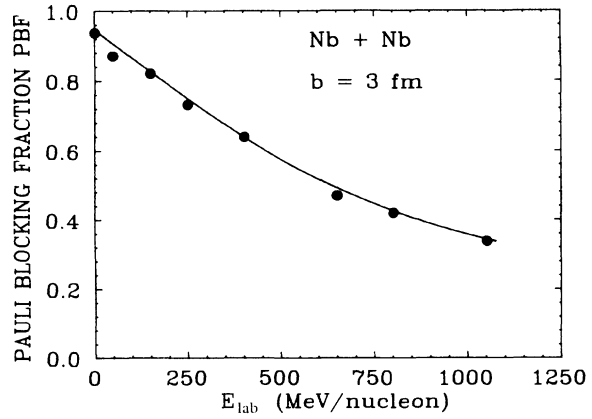

FIG. 15. The dependence of the fraction of Pauli blocked collisions on the bombarding energy.

Observe that the PBF decreases from nearly 95% at zero energy to about 50% at 650 MeV/nucleon. Even at the highest energy studied, $E_{\text{lab}} = 1050$ MeV/nucleon, the PBF is still about $\frac{1}{3}$. This is surprising on first sight because there is so much phase space open to the system. Remind yourself, however, that the Pauli blocking probability is proportional to the inverse phase space density $(1-f)$ squared! Hence, even an f in the participant region of only 0.3 yields a 50% blocking probability. Figure 16 shows how important this quantum in medium effect is for a quantitative calculation of observables, here the flow angle (the same is true, however, also for the other observables, e.g., the pion yield): The flow angle is skewed to much larger values if the Pauli blocking in the participant region is neglected, as is done in all the cascade approaches. Hence, neglect of this important quantal physics results in a gross overestimate of the flow angles. Figure 16 shows also the influence of the other important input into the VUU approach, namely the (local) potential, i.e., the EOS.

It must be emphasized that only as a result of the repulsive potential, i.e., the compression energy in the EOS, do the flow angles deviate drastically from zero. The absolute value of the flow angle reflects the stiffness of the EOS. The impact parameter dependence of the flow angles is shown in Fig. 17 for the hard EOS. Note that the experimentaly observed flow angles in excess of 30° can only be achieved with the hard EOS and for very central collisions, $b \leq 2$ fm, which means that only a small fraction of the inclusive cross section results in large flow effects.[18]

The flow angle increases dramatically with the mass of the system: Figure 18 shows the rise from $\Theta_F \simeq 0°$ to 33°

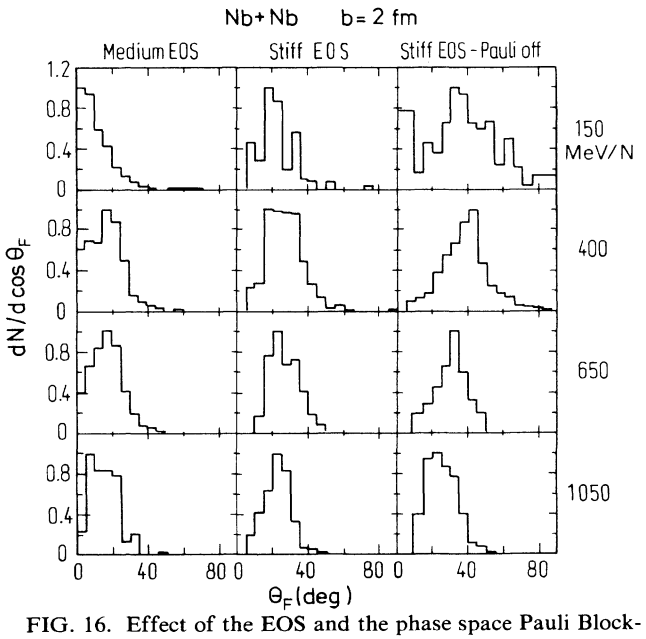

FIG. 16. Effect of the EOS and the phase space Pauli Blocker on the flow angle distribution from 100 to 1000 MeV/nucleon. "Medium" and "stiff" refer to the soft and hard potential of Fig. 1, respectively.

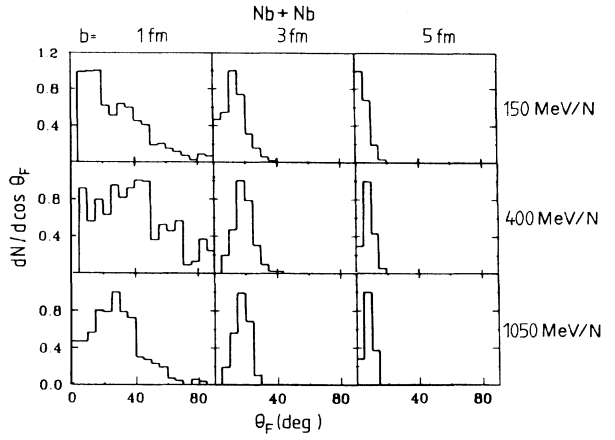

FIG. 17. Same as Fig. 16, but the impact parameter dependence is shown.

when going from Ca + Ca to Au + Au. This finding is qualitatively in accord with the recent experimental observation of the Plastic Ball group.[18]

The Pauli principle and the nuclear EOS are both seen to be important in the accurate prediction of the flow angle. At fixed impact parameter, the flow angle distribution is broader at the lowest energies. Furthermore, the peak flow angle exhibits a maximum at 400 MeV/nucleon.[18]

The quartile of the flow angle distribution for the hard EOS is constant at $\approx 18°$ from 150 to 1050 MeV/nucleon. For the soft EOS the quartile rises from 3° at 150 MeV/nucleon to 13° at 650 MeV/nucleon and then falls to 8° at 1050 MeV/nucleon. The largest *difference* between the equations of state is thus observed at the lowest energy. The problem is that the longitudinal momentum p_z rises as fast or faster than p_x with energy. Thus, even though the transverse momentum p_x increases *greatly* with energy (Fig. 19), the peak and quartile flow angles do not.

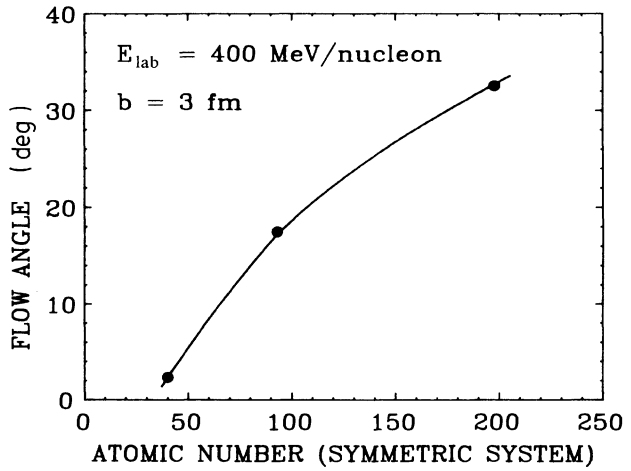

FIG. 18. The dependence of the flow angle on the mass of the system is shown.

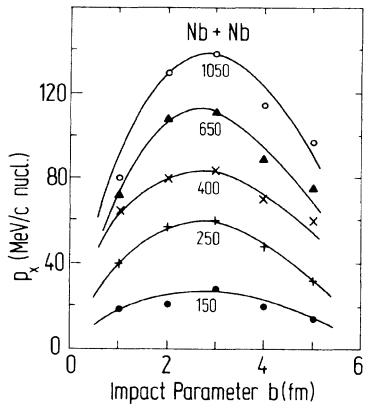

FIG. 19. Energy dependence of the transverse momentum $p_x(y_p)$ impact parameter distribution for the hard EOS.

The flow angle therefore is very sensitive to the stopping power, i.e., the longitudinal momentum degradation. If momentum dependent interactions are used,[6] less stopping and therefore smaller flow angles result. This is so in spite of the fact that the transverse momentum transfer is nearly identical for hard equations of state, be they composed of a hard local potential alone or of a hard local potential plus a momentum dependent term, which both yield the same EOS.[6]

The transverse momentum spectra $p_x(y)$ have an S-shaped form, peaking at projectile and target rapidity, respectively.[4,17] Figure 19 shows the impact parameter dependence of the maximum of the $p_x(y_p)$ distributions for various bombarding energies for the system Nb + Nb, using the hard potential. The transverse momentum varies from zero at $b=0$ for symmetry reasons to a maximum at intermediate impact parameters to zero again for peripheral interactions. Furthermore, there is a strong energy dependence: The peak at intermediate impact parameters $p_x^{\max}(y_p)$ increases from 20 MeV/c/nucleon at $E_{\text{lab}}=150$ MeV/nucleon to 140 MeV/c/nucleon at $E_{\text{lab}}=1050$ MeV/nucleon.

Experimentally, one finds $p_x(y_p)=80$ MeV/c/nucleon for Nb(650 MeV/nucleon) + Nb for 75% of the max-

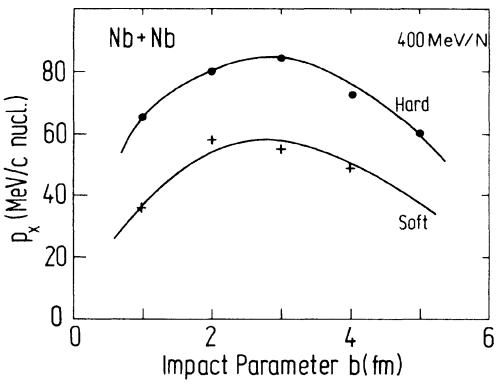

FIG. 20. Impact parameter dependence of the transverse momentum $p_x(y_p)$ for the H and S EOS.

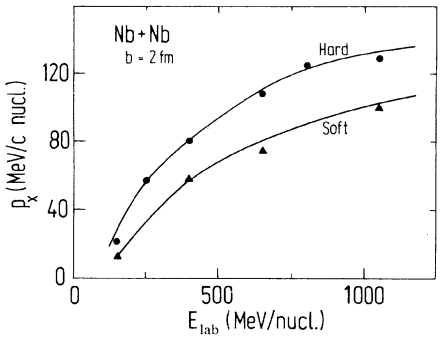

FIG. 21. Energy dependence of $p_x(y_p)$ at an impact parameter close to the maximum for soft and hard EOS.

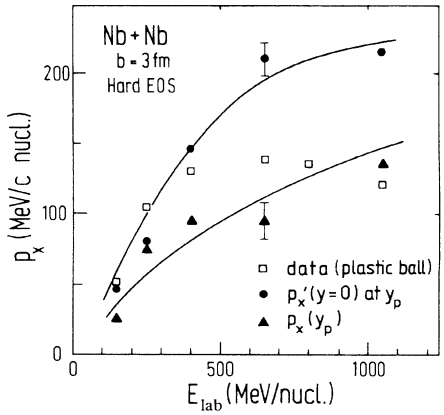

FIG. 22. Extrapolated central transverse momentum $p_x^{extr}(y_p)$ compared to the actual value of $p_x(y_p)$. The extrapolated data are also shown (Ref. 19).

imum multiplicity.[19] One cannot directly compare this to Fig. 19, without an association of b and M. However, if one plots $p_x(y_p)$ vs multiplicity,[19] then the peak values can be compared.

How sensitive is p_x to the nuclear equation of state? We have already seen that for Ar(1.8 GeV/nucleon) + KCl, the current experimental data[17] seem to favor a stiff EOS.[4] Figure 20 shows the sensitivity of the maximum transverse momentum versus impact parameter to the EOS. The largest ($\approx 50\%$) difference between the H and S EOS occurs at the maximum of p_x, i.e., at intermediate impact parameters.

Furthermore, the absolute difference between the p_x values for the H and S EOS increases with energy (Fig. 21): The differences are large as compared with the systematic uncertainties of high statistics experiments, where one has to make sure, though, that the experimental efficiencies are properly taken into account in the theoretical analysis.

This statement becomes obvious when the recent analysis of the flow (p_x) data by the Plastic Ball group[19] is considered: The p_x distributions are most insensitive to spectator contamination at $y_{c.m.} \approx 0$, while at $p_x(y_p)$ this effect is largest. Therefore, the p_x values published by the Plastic Ball group in Ref. 19 have been extracted by fitting a second order polynomial to the slope of the $p_x(y)$ distribution around $y_{c.m.}$. Then the extrapolation of this polynomial to $y = y_p$ has been plotted. This yields a dramatically different p_x value as can be seen in Fig. 22, where the data are compared to the calculated p_x^{max} shown above and to the $p_x(y_p)$ extrapolated with the polynomial prescription introduced in Ref. 19. Observe the large ($\approx 50\%$) difference between the two p_x values. Also note that the data follow nicely the calculation, which used the hard EOS up to $E_{lab} \approx 400$ MeV/nucleon. At higher energies it seems that the data indicate a constant p_x. This could be viewed as a softening of the EOS at higher densities $\rho/\rho_0 \geq 2.5$.

However, another analysis of the same data has yielded consistently higher p_x values,[20] which in fact exceed, particularly for the Au + au system shown in Refs. 2 and 4 for the hard EOS, the theoretical p_x values considerably, indicating that an even stiffer EOS would be required.

In summary, we have seen how in the VUU model the density and temperature develop in a relativistic heavy ion collision. The entropy, pion yields, flow angle, and transverse momentum are seen to saturate just after the moment of maximum compression and temperature of the central region. The transverse momentum near projectile rapidity is an observable with considerable sensitivity to the EOS at intermediate multiplicities. The flow angle distribution is most sensitive to the EOS at 150 MeV/nucleon. A detailed comparison to high statistics data, where all the experimental efficiencies and in-medium effects are taken properly into account in the theory will be needed before one can attempt to extract the nuclear EOS.

ACKNOWLEDGMENTS

J. J. M. acknowledges the receipt of an A. v. Humboldt Fellowship and the hospitality of Professor Greiner and his group at the University of Frankfurt. Stimulating discussions with W. Greiner, G. E. Brown, R. Stock, R. Bock, and H. H. Gutbrod are gratefully acknowledged. This work was supported by Gesellschaft für Schwerionenforschung (Darmstadt) and Bundesministerium für Forschung und Technologie (Bonn, Germany).

*Permanent address: Department of Physics, Muhlenberg College, Allentown, PA 18104.

[1]W. Scheid, H. Mueller, and W. Greiner, Phys. Rev. Lett. 32, 741 (1974); H. Stöcker and W. Greiner, Phys. Rep. 137, 277 (1986).

[2]H. Stöcker, W. Greiner, and W. Scheid, Z. Phys. A 286, 121 (1978); R. Stock, R. Bock, R. Brockmann, J. W. Harris, A. Sandoval, H. Stroebele, K. L. Wolf, H. G. Pugh, L. S.

Schroeder, M. Maier, R. E. Renfordt, and A. Dacal, M. E. Ortiz, Phys. Rev. Lett. **49**, 1236 (1982); J. W. Harris *et al.* Phys. Lett. **153B**, 377 (1985); R. Stock, Phys. Rep. **135**, 259 (1986); D. Hahn and H. Stöcker, Nucl. Phys. **A452**, 723 (1986).

[3]P. Siemens and J. Kapusta, Phys. Rev. Lett. **43**, 1486 (1979); D. Hahn and H. Stöcker, Nucl. Phys. (to be published).

[4]H. Kruse, B. Jacak and H. Stöker, Phys. Rev. Lett. **54**, 289 (1985); J. J. Molitoris and H. Stöcker, Phys. Rev. C **32**, 346 (1985); J. J. Molitoris, D. Hahn, and H. Stöcker, Progr. Part. Nucl. Phys. **15**, 239 (1986); J. J. Molitoris and H. Stöcker, Phys. Lett. **162B**, 47 (1985); G. Bertsch, H. Kruse, and S. DasGupta, Phys. Rev. C **29**, 673 (1984).

[5]H. A. Gustafsson, H. H. Gutbrod, B. Kolb, H. Loehner, B. Ludewigt, A. M. Poskanzer, T. Renner, H. Riedesel, H. G. Ritter, A. Warwick, F. Weik, and H. Wieman, Phys. Rev. Lett. **52**, 1590 (1984); R. E. Renfordt, D. Schall, R. Bock, R. Brockmann, J. W. Harris, A. Sandoval, R. Stock, H. Stroebele, D. Bangert, W. Rauch, G. Odyniec, H. G. Pugh, and L. S. Schroeder, Phys. Rev. Lett. **53**, 763 (1984).

[6]J. Aichelin, A. Rosenhauer, G. Peilert, H. Stöcker, and W. Greiner, Phys. Rev. Lett. **58**, 1926 (1987). The importance of in-medium corrections (effective momentum dependent nucleon mass, effective cross sections) to VUU has been pointed out by various authors; see, for example, R. Malfliet, B. ter Haar, and W. Botermaus (unpublished), and Phys. Rev. Lett. **56**, 1237 (1985); Phys. Lett. **172B**, 10 (1986); T. L. Ainsworth, E. Baron, G. E. Brown, J. Cooperstein, and M. Prakash, Nucl. Phys. **A464**, 740 (1987); C. Gale *et al.* (unpublished).

[7]B. Friedman and V. R. Pandharipande, Nucl. Phys. **A361**, 502 (1981).

[8]E. Baron, J. Cooperstein, and S. Kahana, State University of New York at Stony Brook report, 1985.

[9]J. Cugnon, T. Mizutani, and J. Van der Meulen, Nucl. Phys. **A352**, 505 (1981).

[10]J. J. Molitoris, H. Stöcker, H. A. Gustafsson, J. Cugnon, and D. L'Hôte, Phys. Rev. C **33**, 867 (1986).

[11]R. Hagedorn, Academic Training Program Lecture, European Organization for Nuclear Research (CERN) 1970—71, Geneva (unpublished).

[12]K. G. R. Doss *et al.*, Phys. Rev. C **32**, 116 (1985).

[13]G. Bertsch and J. Cugnon, Phys. Rev. C **24**, 2514 (1981).

[14]K. K. Gudima, V. D. Toneev, G. Roepke, and H. Schulz, Phys. Rev. C **32**, 1605 (1985).

[15]W. Rauch, Ph.D. thesis, University of Frankfurt, 1986. J. W. Harris *et al.*, Phys. Rev. Lett. (to be published).

[16]M. Gyulassy, K. A. Frankel, and H. Stöcker, Phys. Lett. **110B**, 185 (1982).

[17]P. Danielewicz and G. Odyniec, Phys. Lett. **157B**, 146 (1985).

[18]H. G. Ritter, K. G. R. Doss, H. A. Gustafsson, H. H. Gutbrod, K. H. Kampert, B. Kolb, H. Löhner, B. Ludewigt, A. M. Poskanzer, A. Warwick, and H. Wieman, Nucl. Phys. **A477**, 3c (1985).

[19]K. G. R. Doss *et al.*, Phys. Rev. Lett. **57**, 302 (1986).

[20]K. H. Kampert, Ph.D. thesis, Universität Münster, 1986.